Macro-physical, optical and radiative properties of tropical cirrus clouds and its temperature dependence at Gadanki (13.5° N, 79.2° E) observed by ground based lidar

Reji K Dhaman[a,b]*, M Satyanarayana[b,c]*, Krishnakumar V[b,d], V P Mahadevan Pillai[b], Jayeshlal G S[b], K Raghunath[e] & M Venkat Ratnam[e]

[a]Department of Basic Science &Humanities, Indian Naval Academy, Kannur 670 310, India

[b]Department of Optoelectronics, University of Kerala, Trivandrum 695 581, India

[c]VNR Vignana Jyothi Institute of Engineering and Technology, Hyderabad 500 090, India

[d]Department of Physics, St.Gregorios College, Kollam 691 531, India

[e]National Atmospheric Research Laboratory, Tirupati 517 502, India

The macro-physical and optical properties of cirrus clouds and its temperature dependencies have been investigated at the National Atmospheric Research Laboratory (NARL; 13.5° N, 79.2° E), Gadanki, Andhra Pradesh, India; an inland tropical station during the period of observation January to December 2009 using a ground based pulsed monostatic lidar system data and radiosonde measurements. Based on the analysis of measurements the cirrus macrophysical properties such as occurrence height, mid cloud temperature, cloud geometrical thickness, and optical properties such as extinction coefficient, optical depth, depolarization ratio and lidar ratio have been determined. The variation of cirrus macrophysical and optical properties with mid cloud temperature have also been studied. The cirrus clouds mean height has been generally observed in the range of 9-17 km with a peak occurrence at 13-14 km. The cirrus mid cloud temperatures were in the range from -81 °C to -46 °C. The cirrus geometrical thickness ranges from 0.9-4.5 km and 56% of cirrus occurrences have thickness 1.0 -2.7 km. The monthly cirrus optical depth ranges from 0.01-0.47, but most (>80%) of the cirrus have values less than 0.1. The monthly mean cirrus extinction ranges from 2.8E-06 to 8E-05 and depolarization ratio and lidar ratio varies from 0.13 to 0.77 and 2 to 52 respectively. The temperature and thickness dependencies on cirrus optical properties have also been studied. A maximum cirrus geometrical thickness of 4.5 km is found at temperatures around – 46 °C with an indication that optical depth increases with increasing thickness and mid cloud temperature. The cloud radiative properties such as outgoing long-wave radiation (OLR) flux and cirrus IR forcing are studied. OLR flux during the cirrus occurrence days ranged from 348-456 W/m^2 with a low value in the monsoon period. The cirrus IR forcing varied from 3.13 – 110.54 W/m^2 and shows a peak at monsoon period.

Keywords: Cirrus cloud, Lidar, Extinction, Optical depth, Depolarisation ratio, Lidar ratio

1 Introduction

Among the different cloud types, high altitude, thin and wispy cold clouds consisting of non-spherical ice crystals namely, cirrus clouds are the most commonly occurring cloud type and many studies reveal that cirrus clouds play a vital role in the radiation budget or radiance balance of the earth-atmospheric system[1-3]. Cirrus clouds are widely spread in the upper troposphere and they cover about 30% of the total earth's surface[4]. Cirrus clouds play a vital role in the earth's climate system by their capability of two radiative effects namely, green-house effect (by trapping outgoing infrared radiation, leading to a warming of the system) and albedo effect (by reflecting incoming solar radiation back to space, leading to a cooling of the system)[5,6]. These radiative effects are strongly depending on the cirrus macrophysical and optical properties. Optically thin cirrus clouds usually cause positive radiative forcing at the top of the atmosphere and they warm the climate system, whereas optically thick cirrus produces negative radiative forcing which cool the climate[7]. In order to quantify the role of optically thin cirrus clouds on the atmosphere, the vertical structure of clouds with certain macrophysical parameters such as cloud occurrence heights, cloud geometrical thickness and optical properties such as cloud extinction, optical depth, depolarization ratio and lidar ratio and radiative properties such as outgoing long-

*Corresponding author (E-mail: rejikdhaman2007@gmail.com, drsatyanarayana.malladi@gmail.com)

wave radiation (OLR) flux and cirrus IR forcing are to be characterized and the monthly and seasonal variation of these parameters with the mid cloud temperature are to be understood.

Two mechanisms are thought for the formation of cirrus clouds; transportation of large amounts of ice/liquid water to the upper troposphere by cumulonimbus clouds and in situ formation of ice crystals by synoptic scale uplift, which generate nucleation of ice crystals by homogeneous freezing of sulphuric acid or nitric acid haze particles[8].

Ground based lidar technique has become an effective tool for monitoring and characterizing cirrus clouds as well as to investigate the physical properties of cloud composing particles because of the high spatial and temporal resolution it provides at fixed locations. Using ground based lidar measurements, extensive studies have been carried out by various research groups regarding macro- and microphysical and optical properties as well as radiative effects of cirrus clouds over tropics[9-12]. It should be highlighted that cirrus climatology observed by a ground based lidar over one fixed location cannot be considered globally representative. Significant uncertainties in cloud characteristics will occur from one region to another and the clouds representation in climate models require more attention. Characterizing the vertical distribution of clouds with better spatial and temporal resolutions, including the macro-and microphysical as well as optical properties of cirrus clouds at different geographical locations is vital for understanding and quantifying the role of clouds in climate change and for developing accurate weather climate models[13].

The experimental site National Atmospheric Research Laboratory (NARL), Gadanki (13.5° N, 79.2° E), is a tropical rural station, situated in the southern peninsular India and is about 120 km inland from the east coast of India. To understand the morphology and the effect of cirrus clouds, ground based lidar observations were carried out at NARL, during the period of observation from January to December 2009. The macrophysical and optical properties of cirrus clouds over Gadanki are discussed here in detail.

2 Instrumentation

The lidar system employs a Nd: YAG Pulsed Laser operated at its second harmonic of 532 nm with a maximum pulse energy of 550 mJ. The laser pulse-width is 7 ns with a pulse repetition rate of 20 Hz. The receiver system employs a 350 mm diameter Schmidt-Cassegrain-type telescope with a FOV of 1 mrad, which is used to study the altitude structure of atmospheric aerosols employing the Rayleigh and Mie scattered signal up to 40 km. The receiver of this lidar system has depolarization measurement capability. A polarized beam splitter splits the beam into co-polarized and cross-polarized components. These two signals are recorded by two independent and identical photo multiplier tube (PMT) channels operated in photon counting mode. These two channels are referred to as P (co-polarized) and S (cross-polarized) channels, respectively. The photon counting signals are sent to an MCS-Plus channel for signal analysis. These data in both the channels are acquired with a dwell time of 2 μs (corresponding to an altitude resolution of 300 m) over 1024 range bins and summed over 250 s (5000 transmitted pulses) to achieve a good signal-to-noise ratio up to altitudes greater than 30 km.

3 Data Analysis

The lidar system at Gadanki is operated during clear sky conditions and free from low level clouds; typically about 4-6 h of observations are made during each observation day at night from 22:00 to 05:00 Indian Standard Time (IST; corresponding to 82.5° E). There are either less or no observations during the monsoon period mainly due to limitations of optical system availability for operating during clear sky conditions. Measurements are carried out during the period of observation from January to December 2009. The cirrus cloud data observed during the 16 days out of the 21 days of observation are used for the investigations on cirrus clouds. Simultaneous data on temperature are taken from radiosonde experiments conducted at the station during the same period. Here we have considered the cold point tropopause for identifying the tropopause height.

The backscattered signal obtained from the lidar is first corrected for background noise counts and then range normalized. Each of the lidar pulse sent into the atmosphere, the received backscatter signal includes the scattering from background aerosol and contribution of cirrus cloud if it is present, during that time in the atmosphere. In the absence of any cloud the backscattered signal falls off gradually depending up on the background aerosol properties. By observing the lidar data one can easily detect the presence of cirrus cloud by studying the lidar

backscattered signal. The relative values of the backscattered signal profile from the background aerosol and the region where the cloud is present will unambiguously indicate the presence of a cirrus cloud. Thus the cirrus clouds can be detected by noting down a sudden increase in the backscatter data in the region of the cloud relative to background aerosol signal.

3.1 Macro-physical properties of cirrus

The cirrus macrophysical properties such as occurrence heights (cloud base, cloud mid and cloud top), cloud geometrical thickness, and cirrus height from the tropopause are determined from the lidar datasets. The cloud mid height is taken as the mid-point between the cloud base and top height of each cirrus layer. The cloud geometrical thickness is measured as the difference between the cloud top and base heights of cirrus layer. The cloud base, mid and top temperatures are taken from the radiosonde measurements for the corresponding height. Each cirrus layer level from the tropopause is determined as the difference between the tropopause height and the mid cloud height.

3.2 Optical properties of cirrus

Optical properties of cirrus, which are essential for the cloud radiative effects, can be derived from LIDAR observations. The cloud extinction coefficient are obtained by the widely used (Klett, 1981) Klett LIDAR inversion methods[14]. A range independent LIDAR ratio (LR) is used in these techniques for retrieving the extinction coefficients. Making use of the LIDAR system constants and from the measured backscattered signal power, the extinction coefficient of the clouds is determined by inverting the LIDAR signals as described by Klett.

The optical depth (τ_c) of the cirrus cloud can be obtained from LIDAR data using the equation:

$$\tau_c = \int_{h_{base}}^{h_{top}} \alpha(h)dh$$

where $\alpha(h)$ is the extinction coefficient within the cloud region, which extends from cloud base (h_{base}) to cloud top (h_{top}). Based on optical depth, cirrus clouds are classified into sub-visual cirrus (SVC) ($\tau_c < 0.03$), optically thin cirrus (TC) ($0.03 < \tau_c < 0.3$) and dense cirrus (DC) or opaque clouds ($0.3 < \tau_c < 3.0$)[15].

The linear depolarisation ratio (LDR) is a function of altitude, temperature, and humidity distribution within the cloud. Depolarization measurements can provide insight into the distribution of ice and water within clouds and help in the investigation of cloud formation and dynamics[15,16]. The linear depolarisation factor $\delta(h)$ is related to backscattering coefficients that are estimated using lidar signals from the co-polarized (*P*) and cross-polarized (*S*) channels, respectively and is estimated using the equation:

$$\delta(h) = \frac{\beta_s(h)}{\beta_p(h)}$$

where $\beta_s(h)$ and $\beta_p(h)$ are the backscattering coefficients of *S* and *P* channels[17]. Scattering from a spherical particle for an incident polarized beam has no significant depolarisation and this is applicable to water particles in clouds. The water in the cloud in crystalline form and the shape of the crystal contribute for the depolarisation.

The extinction-to-backscatter ratio, usually termed as lidar ratio (LR) is an important parameter to obtain the nature of cloud particles while studying the optical properties. The LR values in combination with LDR are used to suggest the type of ice crystals present in clouds. The altitude dependent LR value was calculated from the method described in detail by Satyanarayana *et al.*[18]

3.3 Radiative properties of cirrus

Many investigators[3,7,17,19,20] have attempted for the parameterization of cirrus radiative properties based on the cloud parameters like optical depth, particle shape and size distribution, ice water content etc. Here we are presenting the cirrus radiative forcing with respect to cloud optical depth, by considering a single layer cloud structure. The outgoing long-wave radiation (OLR) flux F (W/m^2) is calculated by using the equation,

$$F = \sigma\left(T_s^4 - T^4\right)exp\left(-D\tau_c / C\right) + \sigma T^4$$

where τ_c is the cloud optical depth, σ is the Stephan-Boltzmann constant ($\approx 5.67 \times 10^{-8}$ Js^{-1} m^{-2}K^{-4}), T_s is the surface temperature ($T_s \sim 300$ K over tropical station Gadanki), T the cloud temperature, D is the diffusivity factor (1.66) and C is a constant (~2). Depending on the cloud altitude and the optical depth OLR flux will vary for sub-visual, thin and dense cirrus. The cirrus IR forcing is calculated as, $f_c = \sigma T_s^4 - F$, where the initial term represents the clear sky OLR flux.

4 Results and Discussion

Lidar observations taken during the period January 2009 to December 2009 on clear sky nights are used for the present study. Out of the lidar data collected for 21 nights during the observation period, cirrus clouds are detected for 16 nights (76%). The statistics is in agreement with the observations by Sassen *et al.*[9], who reported more than 50% of cirrus clouds in the tropics. Lidar signals summed for 250 s yield one lidar profile and are used to determine the frequency of observation of cirrus clouds. Figure 1 shows an overview of the evolution of the geometrical structure of three types of cirrus clouds viz, sub-visual, thin and dense cirrus with its cloud base and top and the hourly variation with altitude of the logarithmic scale of range squared signal observed during the cirrus occurrence days. The layered cloud has been observed and shown.

4.1 Macro-physical properties of cirrus

Figure 2(a-e) represents the occurrence/frequency distribution of cloud base, top, mid altitudes, cloud thickness and mid-cloud temperature. Cirrus cloud base altitude ranged from 8.7−16.8 km including the layered clouds and mostly (93.8%) the base altitude lay between 11−16 km. The cloud base altitudes have a maximum distribution (25%) between 11–12 km. Figure 2(b) represents the occurrence distribution of cloud top altitude, indicating that cloud top altitude ranged from 10.2–18.3 km and 81.3% of measurements it lie in 13–17 km, which is in good agreement with the values reported by Comstock *et al.*[10], over a tropical island, who found it to be around 16 km and by Seifert *et al.*[11], who found it to be in the range 13–15 km over another tropical island. The top altitudes have a maximum distribution at 14–15 km. Figure 2(c) indicates the cloud-mid altitude
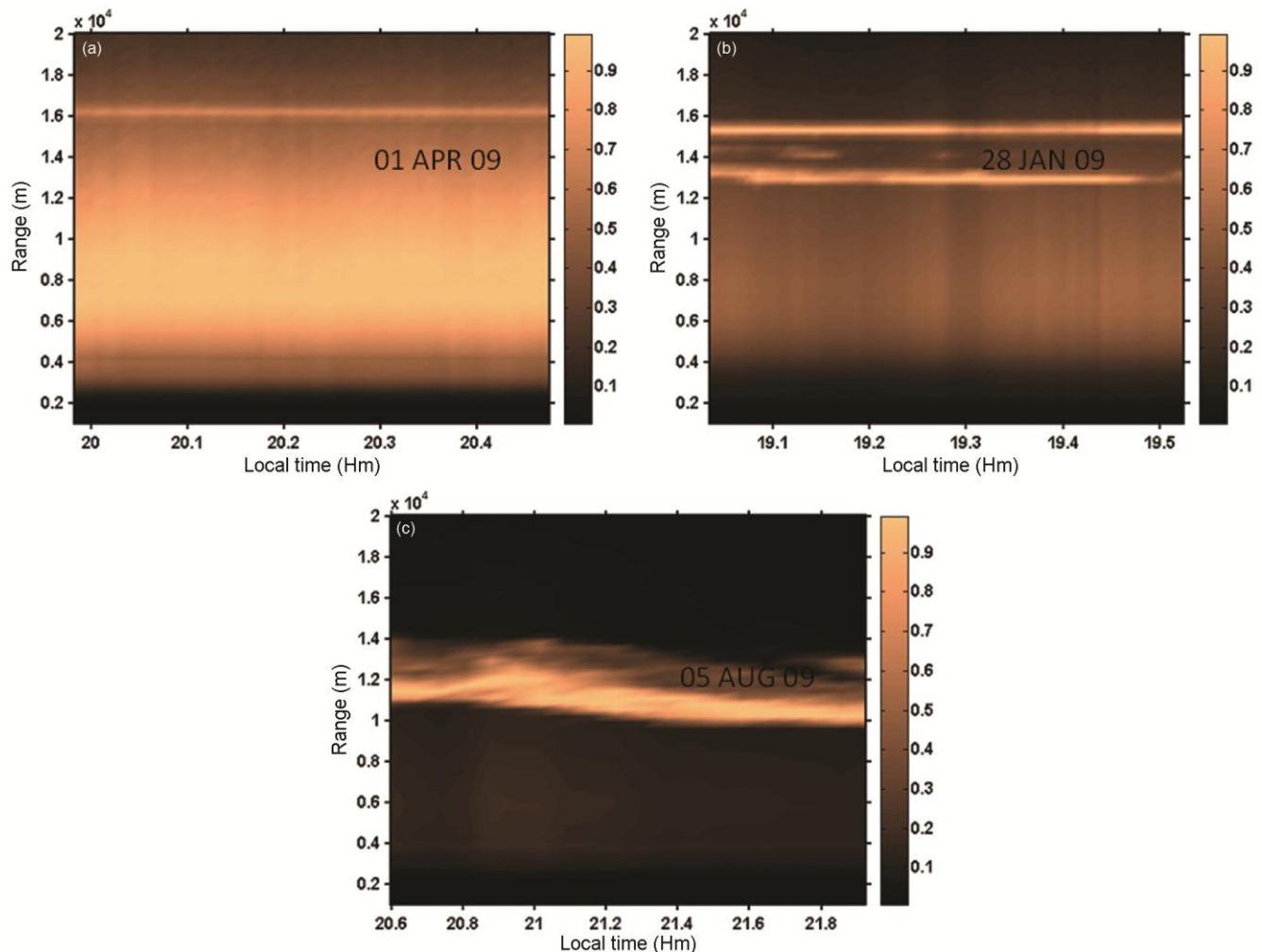
Fig. 1 − Altitude versus time display of cirrus clouds (a) sub-visual, (b) thin and (c) dense observed during the cirrus days from lidar profiles
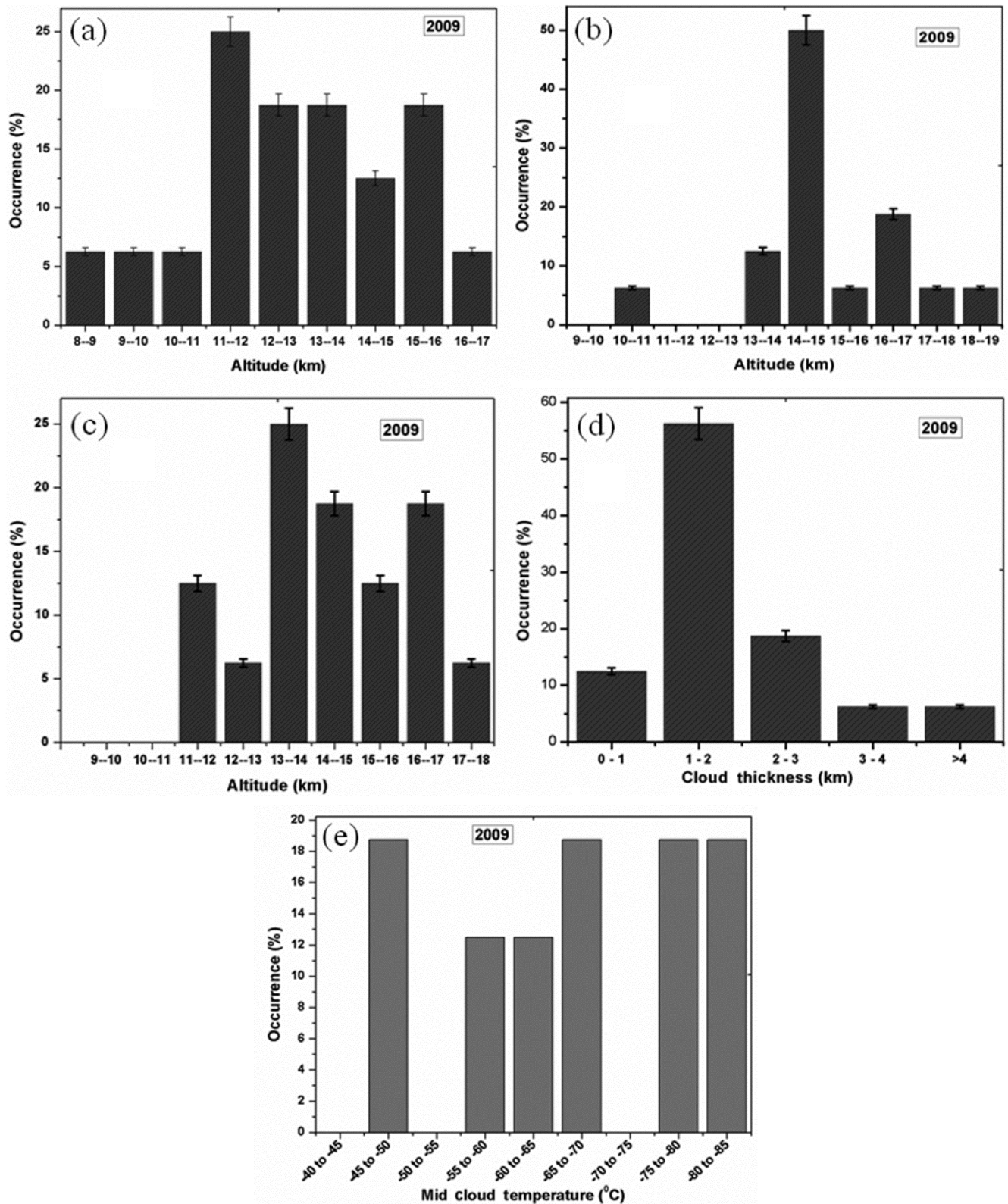
Fig. 2 − Frequency distribution of cirrus occurrence with (a) base altitude, (b) mid altitude, (c) top altitude, (d) geometrical thickness and (e) mid-cloud temperature

distribution which ranged from 9.6–17.7 km with a maximum distribution at 13–14 km. The cirrus is generally found to occur somewhat close to the tropopause. The probability distribution of cloud geometrical thickness is presented in Fig. 2(d). The geometrical thickness was confined to a range of 0.9–4.5 km. About 75%, the thickness of cirrus clouds was 1.0–2.7 km. The clouds having the low values of thickness (≤1.2 km) are generally optically TC and the clouds having optical depth <0.03 are SVC. The maximum geometrical depth observed were 3.3 km and 4.5 km in the monsoon period. Details of the observation days, cloud base, mid and top altitudes along with cloud thickness, tropopause height, distance of cirrus from tropopause and temperature during the days of observation are given in Table 1. All temperature data are obtained from radiosonde launched near simultaneously during the days of observation.

Cirrus clouds detected near the tropopause are usually thin and mostly sub-visual. The cold point tropopause (CPT) height is ~17.34 km with temperature -82 °C. It is seen that some of the cirrus clouds occur near and sometimes above the CPT. Cirrus mid-cloud temperature ranged from -85 °C to -28 °C, which is close to the values reported by Das *et al.*[21], over Chung-Li, a tropical station with mid-cloud temperatures between -80 °C to -30 °C. The minimum tropopause temperature (-83 °C to -63 °C) occurs over the tropics, which favors the frequent formation of cirrus and indicates the dominance of ice crystals in the cirrus clouds. The cirrus clouds which are much below the tropopause are having temperatures and the ice crystal compositions are entirely different from those clouds that occur very close to the tropopause.

Figure 3 represents the monthly variation of cirrus cloud base, mid, top altitudes and tropopause height during the period of observation. No seasonal behavior can be attributed with this limited data. However the months corresponding to the date of observations are indicated. The four prominent seasons of the station are the south west (SW) monsoon (June to August), north east (NE) monsoon (September to November), summer (March to May) and winter (December to February). The cirrus cloud base, mid and top height shows peak values in February and October. When the cirrus base is at lower height, the geometrical thickness become wider which can be attributed to anvil cirrus that are formed

Table 1 − Cirrus clouds macro-physical properties observed during the period of observation

Observation day	No of layered clouds	CBH (km)	CMH (km)	CTH (km)	CBT (°C)	CMT (°C)	CTT (°C)	CGT (km)	Tropopause height (km)	Distance from tropopause (km)
21 January	1	15.6	16.2	16.8	-76	-79	-85	1.2	17.4	-1.2
28 January	1	14.7	15.3	15.9	-73	-78	-83	1.2	17.3	-2.0
	2	12.3	12.9	13.8	-53	-58	-66	1.5	17.3	-4.4
11 February	1	15.9	16.5	17.1	-77	-81	-85	1.2	17.5	-1.0
04 March	1	13.2	14.1	14.7	-60	-67	-73	1.5	17.8	-3.7
01 April	1	15.6	16.2	16.8	-75	-79	-83	1.2	17.7	-1.5
29 April	1	12.6	13.2	13.5	-54	-58	-61	0.9	18.0	-4.8
	2	11.4	12	12.6	-45	-50	-54	1.2	18.0	-6.0
13 May	1	13.8	14.1	14.7	-62	-66	-69	0.9	17.2	-3.1
03 June	1	12.0	13.2	14.1	-48	-57	-66	2.1	16.5	-3.3
22 July	1	10.5	12.0	13.8	-35	-49	-62	3.3	16.7	-4.7
	2	8.7	9.6	10.2	-21	-28	-32	1.5	16.7	-7.1
05 August	1	9.6	11.1	14.1	-28	-46	-63	4.5	17.1	-6.0
16 September	1	12.0	13.8	14.7	-49	-60	-71	2.7	18.0	-4.2
07 October	1	16.8	17.7	18.3	-80	-81	-80	1.5	18.1	-0.4
21 October	1	14.7	15.6	16.2	-73	-75	-82	1.5	16.4	-0.8
18 November	1	12.0	12.9	14.4	-50	-60	-71	2.4	17.1	-4.2
25 November	1	13.2	14.1	14.7	-59	-66	-72	1.5	17.8	-3.7
30 December	1	12.9	13.8	14.7	-58	-66	-74	1.8	16.9	-3.1
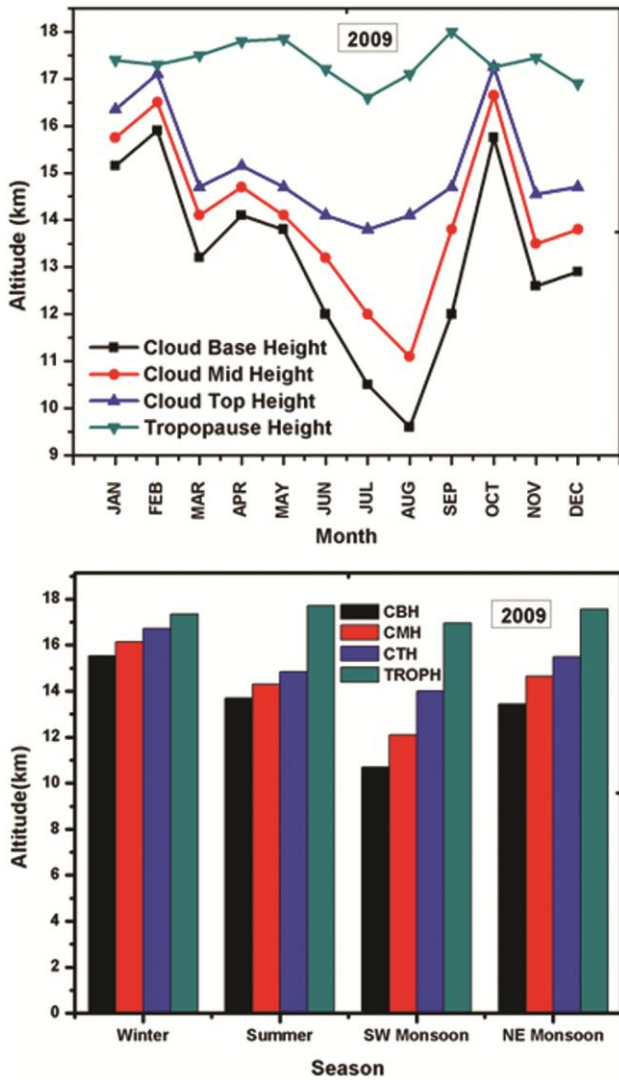
Fig. 3 − Monthly and seasonal variation of cirrus clouds base, mid, top and tropo-pause height

Fig. 4 − (a) Monthly mean cirrus geometrical thickness with mid-cloud temperature and (b) cloud mean altitude with mid-cloud temperature

from cumulonimbus cloud by deep convection. When the cloud base is at high altitude the geometrical thickness decreases with increasing base height and they become thin and are close to the tropopause. The tropopause layer showed the common behavior of high altitude in the summer and low altitude towards the winter. The average base of cirrus clouds is found to be lowest during June-August (SW monsoon), with a value of 10.7±1.99 km. However, minimum cloud top height is also observed on July, with a mean value of 14±1.15 km. During winter, SVC occurrence is mostly high compared to TC and DC, while the occurrence of TC and DC is greater during the monsoon periods (June to September).

Figure 4(a) represents the plot of mid-cloud temperature with the cirrus geometrical thickness

during the observation period. The clouds having the low values of geometrical thickness (≤1.2 km) are generally optically TC and the clouds having optical depth <0.03 are SVC. It is observed that most of TC occurs in the range of -60 °C to -85 °C and the SVC occur at temperatures lower than -65 °C. The DC occurs on the temperature range of -46 °C, with geometrical thickness of 3.3 km and 4.5 km during the SW monsoon, which is in agreement with Norris *et al.*[22], who reported that the maximum thickness occurs when the temperature is around -50 °C and drops off on either side of -50 °C at mid latitudes. The cloud base is lowered at this temperature which indicates that the cloud thickens is lowering of the cloud base. From Fig. 4(b) it is seen

that the cloud temperature decreases as the cloud mean altitude increases.

4.2 Optical properties of cirrus

Cirrus optical properties, such as extinction coefficient (σ), optical depth (τ_c), depolarisation ratio (δ) and extinction-to-backscatter ratio (commonly termed as lidar ratio, LR) are investigated during the period of observation. Figure 5 represents the vertical profiles of cirrus cloud extinction coefficients for three cloud types, viz., SVC (01 April 2009, summer), TC (28 January 2009, winter and 18 November 2009, NE monsoon) and DC (05 Aug 2009, SW monsoon). Table 2 summarizes the cirrus occurrence day's optical properties.

The extinction coefficient of cirrus clouds was calculated from the lidar data using the Klett's inversion technique. The optical depths of the clouds were calculated by integrating the extinction coefficients in the cloud region, which extends from cloud base to cloud top. Based on optical depth, cirrus

clouds are classified into sub-visual cirrus (SVC) ($\tau_c < 0.03$), optically thin cirrus (TC) ($0.03 < \tau_c < 0.3$) and dense cirrus (DC) or opaque clouds ($0.3 < \tau_c < 3.0$). In this study, monthly mean extinction, σ ranged from 2.84E-06 to 7.99E-05 m^{-1} with an annual mean of 1.79 ± 2.05E-05 m^{-1} which occurs in the month of October and August. From Fig. 5 it is observed that in the case of layered cloud the cloud extinction is more in the top layer than at the bottom. From Table 2, it is seen that the extinction during the months of June, July and August (SW monsoon period) is higher than that of the period from September to November (NE monsoon period). The cloud optical depth ranged from 0.01-0.47 with a mean value of 0.08 ± 0.13, and the occurrence of SVC, TC and DC are 37.5%, 50% and 12.5%. The τ_c variability depends on the composition of cloud and geometrical thickness. τ_c is higher in the monsoon period and the same for geometrical thickness. From Fig. 6 it is clear that τ_c shows a strong dependent tendency with cirrus geometrical thickness. Also τ_c shows dependency with
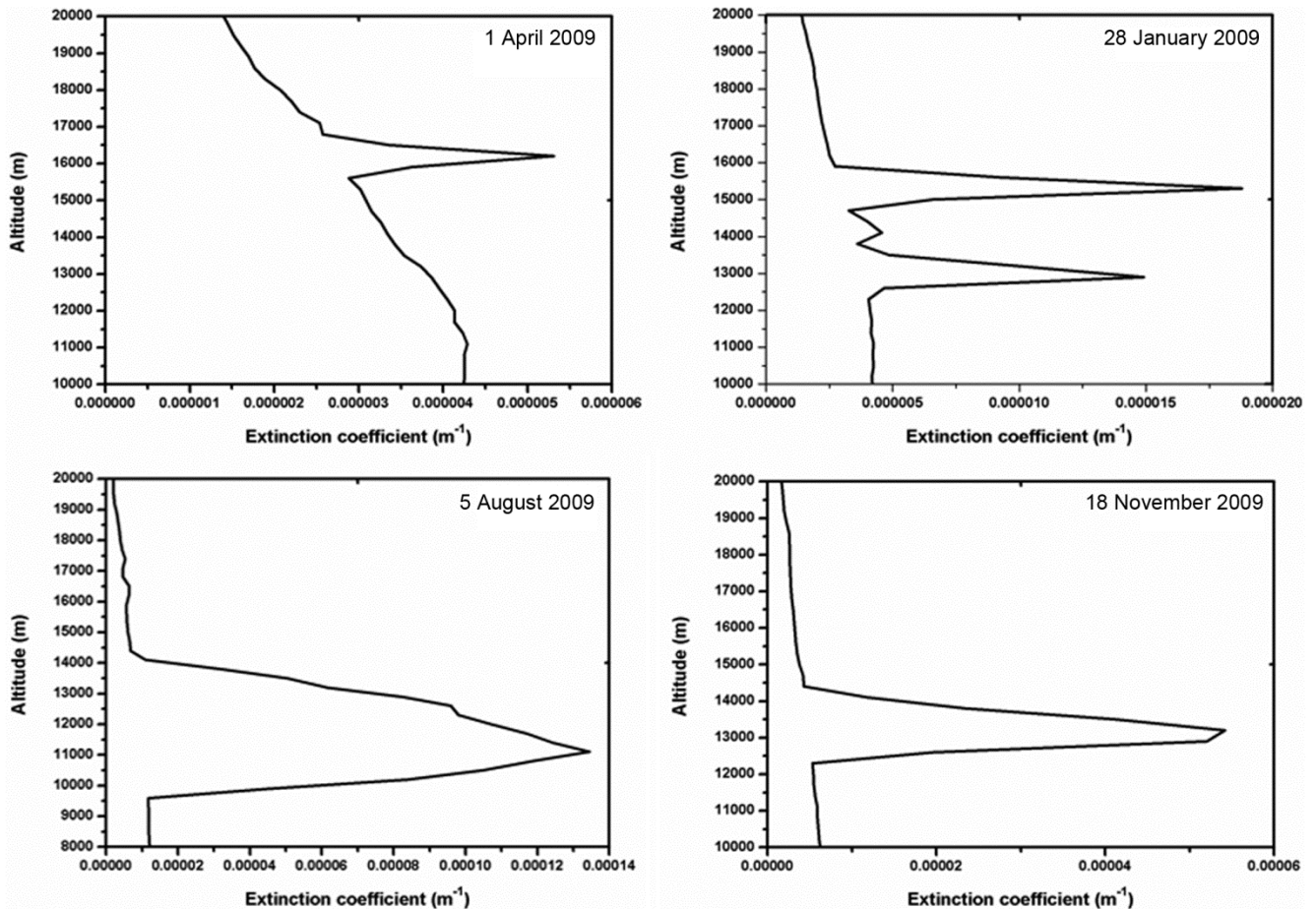
Fig. 5 − Vertical profiles of cirrus cloud extinction coefficient for four days of observation representing four prominent seasons and various cloud types

Table 2 − Cirrus clouds optical properties observed during the period of observation

Date	Extinction (m^{-1}) ×10^{-6}	Mean extinction (m^{-1}) ×10^{-6}	Cloud mid extinction (m^{-1}) ×10^{-6}	Optical depth	LDR	Mean LDR	Lidar ratio	Mean lidar ratio	Type of crystal
21 January (SVC)	3.43–2.96	6.69	14.8	0.02	0.23-0.26	0.32	11.03-12.91	7.76	Mixed phase
28 January (TC)	3.26-2.71	8.11	18.8	0.02	0.25-0.38	0.61	7.49-8.33	4.67	Plate to column
	4.09-3.60	7.00	14.9	0.03	0.19-0.24	0.34	7.80-7.53	5.43	Mixed phase
11 February (TC)	10.2-10.7	14.73	21.9	0.04	0.25-0.30	0.44	47.48-32.36	28.13	Hexagonal column
04 March (TC)	4.54-4.22	11.32	23.0	0.03	0.18-0.38	0.54	20.47-18.69	12.44	Horizontally oriented
01 April (SVC)	2.99-2.82	3.80	5.37	0.01	0.38-0.48	0.57	7.13-6.70	5.60	Hexagonal plate mixed phase
29 April (TC)	7.24-4.52	12.17	19.2	0.04	0.61-0.46	1.09	9.91-18.02	8.52	Randomly oriented
	5.75-7.24	23.67	55.1	0.05	0.09-0.61	0.65	14.67-9.91	6.09	Hexagonal plate Mixed phase
13 May (SVC)	6.49-3.45	15.32	30.1	0.02	0.33-0.30	0.59	10.83-19.55	8.85	Thin plate
03 June (TC)	4.43-36.6	67.84	100.0	0.07	0.42-0.92	0.45	3.21-4.07	2.30	Hexagonal column
22 July (TC)	7.82-3.38	18.91	31.6	0.06	0.17-0.21	0.41	10.09-22.19	6.17	Horizontally oriented
	5.28-6.43	7.23	10.8	0.09	0.01-0.20	0.36	20.98-13.35	14.11	Horizontally oriented thin plate
05 August (DC)	11.9-10.9	79.91	134.0	0.43	0.36-0.19	0.29	36.63-12.15	5.98	Dendrites
16 September (DC)	4.35-3.77	15.49	32.0	0.47	0.06-0.34	0.38	26.61-22.67	10.25	Horizontally oriented
07 October (SVC)	2.35-2.01	2.43	2.79	0.01	0.15-0.14	0.14	12.34-13.38	11.14	Thin plates oriented horizontally
21 October (SVC)	2.93-2.58	3.25	4.01	0.02	0.15-0.14	0.12	14.76-14.21	12.17	Thin plates oriented horizontally
18 NOovember(TC)	5.42-4.29	24.14	52.0	0.03	0.03-0.37	0.45	20.39-24.52	9.14	Horizontally oriented
25 November (SVC)	3.64-3.05	7.52	11.7	0.02	0.14-0.17	0.38	12.43-12.79	7.61	Thin plates oriented horizontally
30 December (TC)	4.03-3.25	10.62	21.8	0.03	0.09-0.16	0.38	3.58-3.52	51.77	Horizontally oriented

mid-cloud height. When the cloud height increased to 11-13.5 km, τ_c decreased and at 13.7 km it show a peak, from 14-16 km τ_c again decreased. τ_c shows a positive correlation with mid-cloud temperature.

Cirrus cloud especially over tropics are mostly composed of non-spherical ice crystals and will cause significant depolarisation. The depolarisation ratio within the cloud is an indicator of cloud microphysical properties. Figure 7 presents the vertical profiles of cirrus cloud depolarisation ratio for three cloud types, viz., SVC (01 April 2009, summer),

TC (28 January 2009, winter and 18 November 2009, NE monsoon) and DC (05 August 2009, SW monsoon). It is seen that during the summer and winter months, depolarisation is high. In 28 January, the cloud depolarization is more in the top layer compared to the bottom layered, and is due to the presence of moderate to heavy rimed ice particles. For the case of DC, the cloud base has low LDR and the temperature is of the range -28 °C to -35 °C, consisting of mixed phase crystals and suggests the presence of reduced ice water content[23, 24].
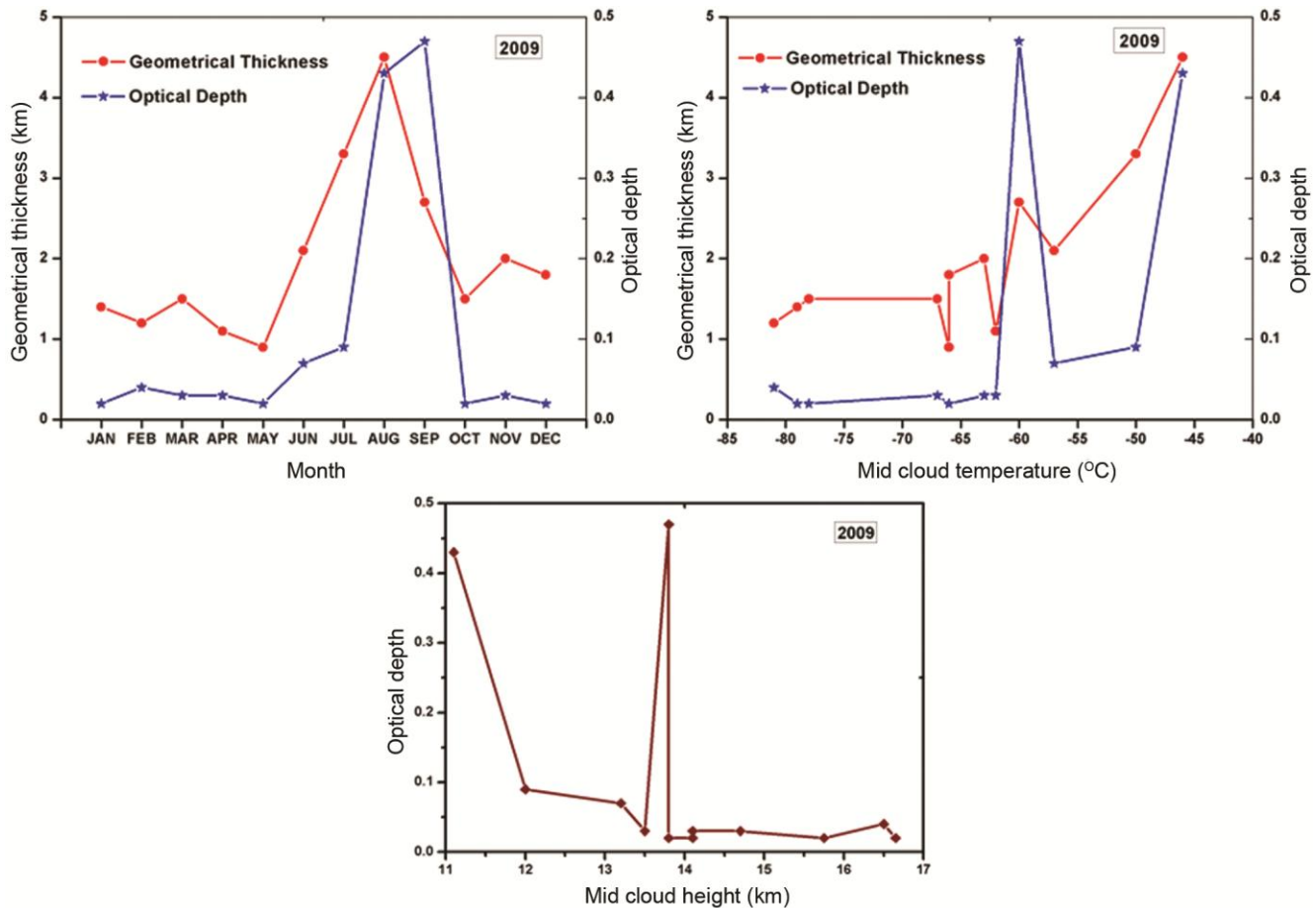
Fig. 6 − Monthly variation of cirrus optical depth and geometrical thickness, its temperature dependence and τ_c with mid-cloud height

From the Table 2 it is seen that monthly mean LDR ranged from 0.12-1.09 with annual mean of 0.45±0.21. The wide variations in the LDR are due to the changes in the cloud composition arising from the nucleation process. The depolarisation ratio is related to the ice crystal shapes. Sassen *et al.*[25] has identified the crystal structure of the clouds, based on the depolarisation value, into randomly oriented hexagonal thin plates, hexagonal thick plates and hexagonal column crystals. Cirrus clouds with low values of extinction coefficient and with low values of depolarization ratio (<0.3) suggests the formation of horizontally oriented ice crystals. Large values of extinction coefficient with high values of depolarization ratio (>0.3) suggest formation of hexagonal plate crystals. Moderate value of extinction and depolarization ratio (around 0.3) suggests the formation of thin plates.

Lidar ratio depends on the ice crystals properties. As shown by Heymsfield and Platt[26], many type of ice crystals exist inside the cirrus clouds at temperatures ≤-50 °C, i.e., around 12 km. Using the range dependent lidar ratio developed by Satyanaryana *et al.*[18], we have found LR for various cloud observations. It is observed that the lidar ratio at cloud bottom and cloud top is higher than mid-cloud. It is found that the lidar ratio varied randomly below 12.5 km. Table 2 shows the cirrus occurrence days LR variations during the period of observation. The wide variations in the LR are due to the changes in the cloud composition.

Figure 8 presents the vertical profiles of cirrus LR for three cloud types, viz., SVC (01 April 2009, summer), TC (28 January 2009, winter and 18 November 2009, NE monsoon) and DC (05 August 2009, SW monsoon). It is clear that in the month of August and November the LR variations are much higher compared to the other two days of observation. Also it is observed that monthly mean LR ranged from 2.30-51.77 sr with annual mean of 11.48±11 sr. Figure 9(a) shows the monthly evolution of extinction of cirrus cloud observed during the year 2009. The
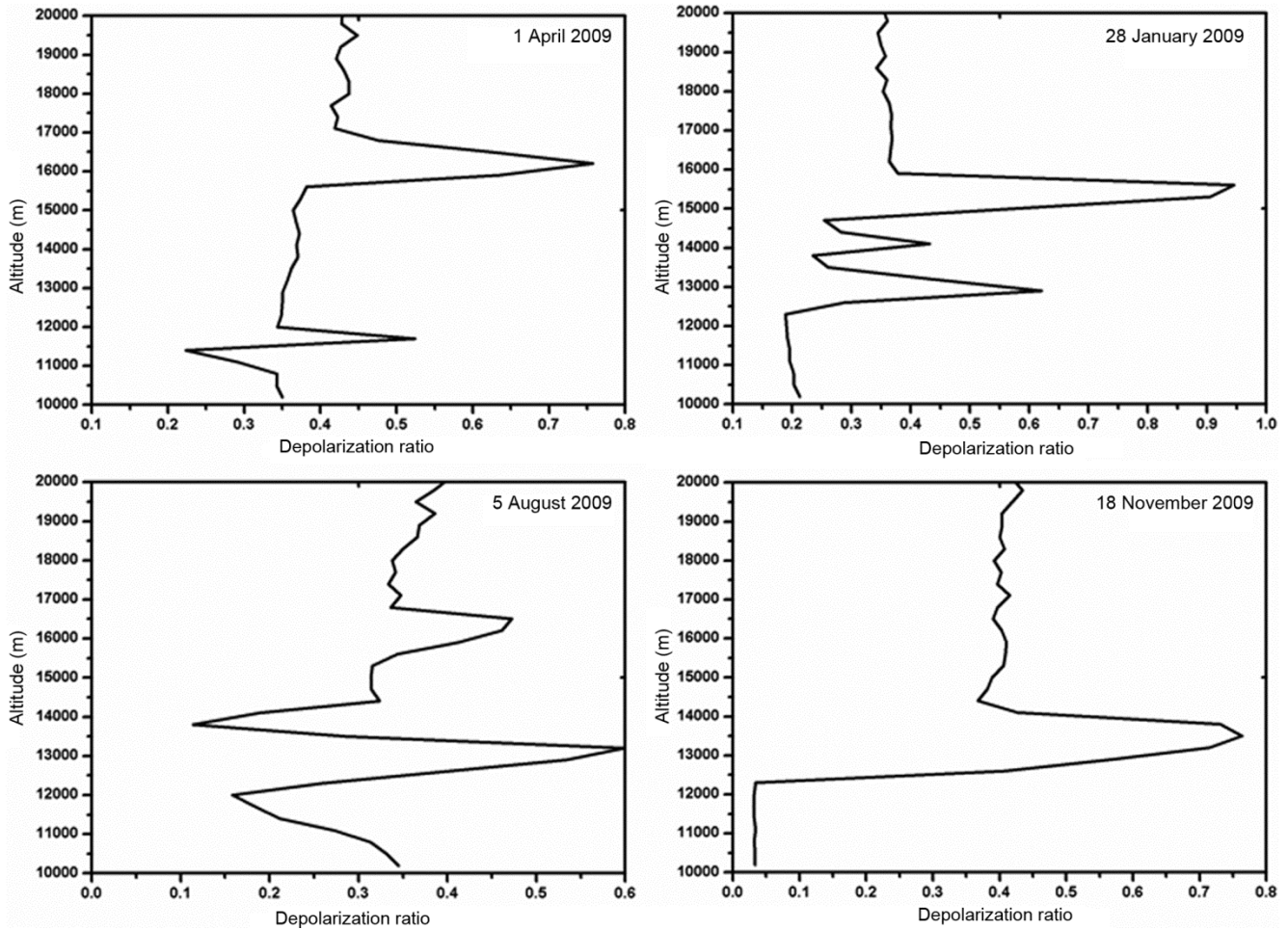
Fig. 7 − Vertical profiles of cirrus cloud depolarization ratio for four days of observation representing four prominent seasons and various cloud types

mean extinction is high in the mid cloud altitude range of 12-13.5 km and above the range the extinction decreases. Figure 9(b) shows the monthly evolution of depolarization ratio of cirrus cloud observed during the year 2009. Figure 9(c) shows the monthly evolution of LR of cirrus cloud observed during the year 2009. The measured values are consistent with the values reported by Platt *et al.*[27] and Sassen *et al.*[15]. The value of extinction coefficient, lidar ratio and depolarization ratio together can be used to get more information regarding the morphology of ice crystals formed.

The cirrus optical properties depend on the temperature and it is necessary to understand the climatology variation of cirrus with temperature for the development of climate models. The dependences of the cirrus optical properties on mid-cloud temperature for every 5 °C interval are shown in

Fig. 10. It is observed that the mean extinction and optical depth show a trend of increase with mid-cloud temperature except the temperature of -50 °C. Hence a positive correlation exists for both optical depth and extinction with the mid-cloud temperature. This is in agreement with the previous results reported[9,15,28,29]. At lower temperatures the ice crystals formed are clusters of hexagonal crystals and at higher temperatures there exist aggregates of crystals including dendrites and rimed forms. It is observed that the depolarisation shows a decrease in the temperature range -60 °C and -45 °C due to the existence of typical ice crystals. The lidar ratio shows a scattered behavior with mid-cloud temperature.

Figure 11 presents the dependence of cirrus optical depth on depolarisation ratio and lidar ratio. It is observed that for the case of SVC, LDR ranged from 0.1 to ~0.6 and LR ranged from 2 to 35 sr, which
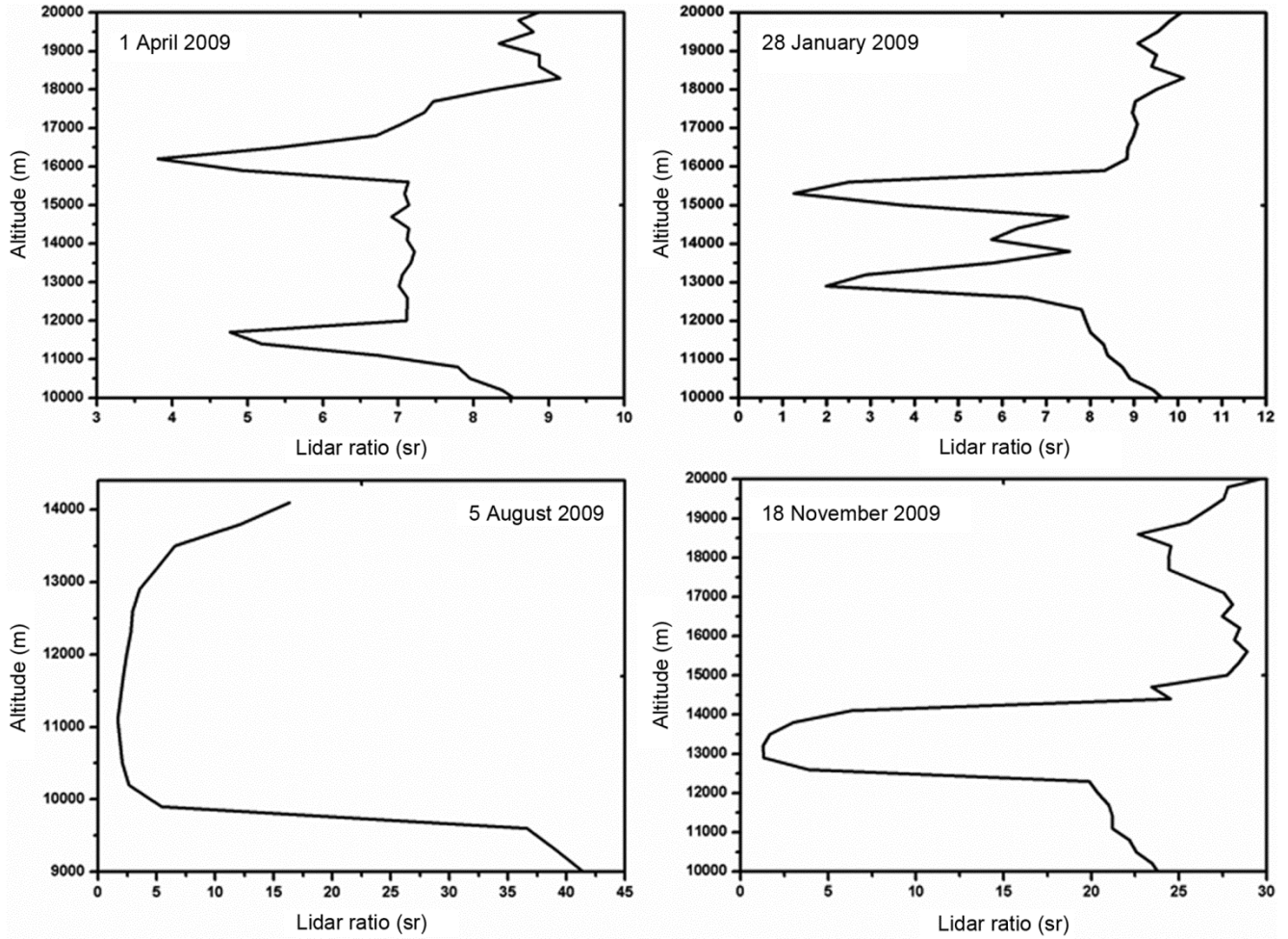
Fig. 8 − Vertical profiles of cirrus cloud lidar ratio for four days of observation representing four prominent seasons and various cloud types
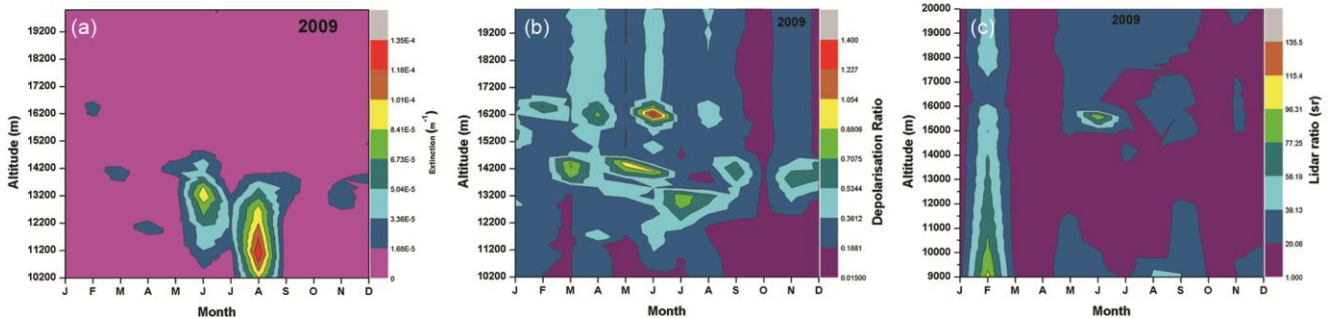
Fig. 9 − Contour plot of the monthly evolution of cirrus clouds (a) extinction coefficient, (b) depolarization ratio and (c) lidar ratio observed in the year 2009

indicates the presence of thin plate ice crystals. For TC, LDR ranged from 0.1 to 0.9, for $\tau_c > 0.15$ the LDR shows a decrease and ranged below 0.14, indicates the presence of hexagonal column for the former and horizontally oriented thin ice crystals for the latter. For the latter case the LR also shows a decrease. For the DC, both LDR and LR are having low values, which show the presence of dendrites and rimed ice particles. Table 3 summarizes the optical properties of SVC, TC and DC optical properties during the period of observation.
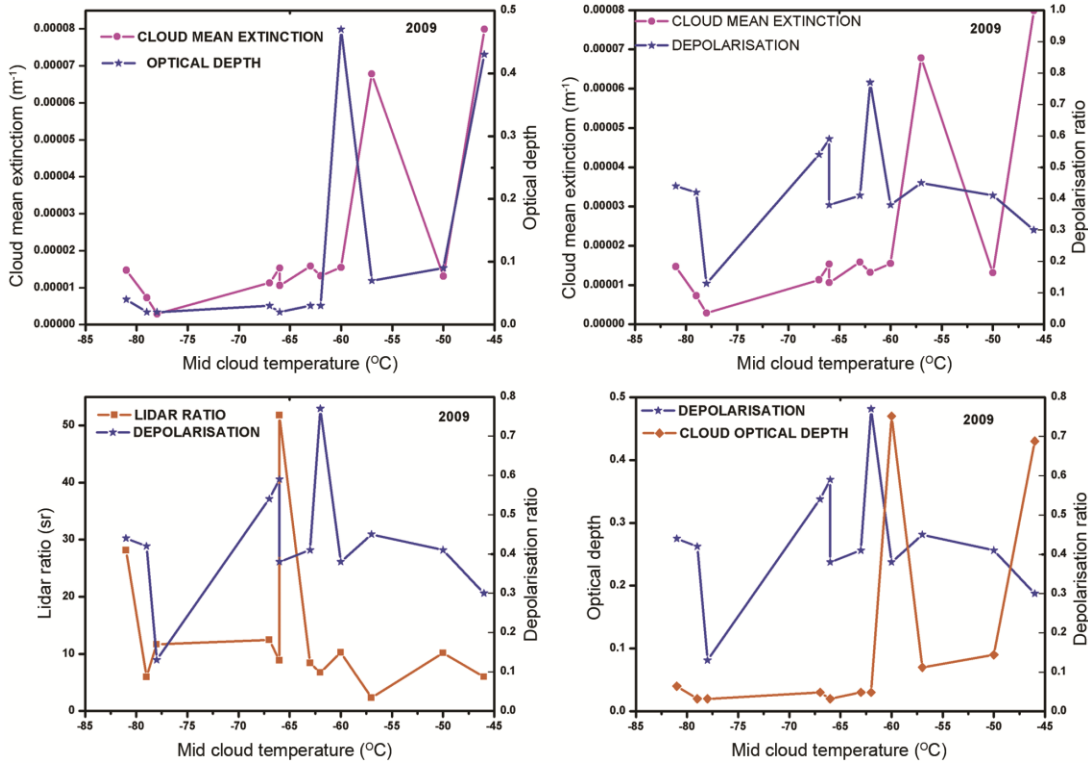
Fig.10 − Cirrus cloud optical properties variation on mid-cloud temperature for every 5 °C interval during the period of observation
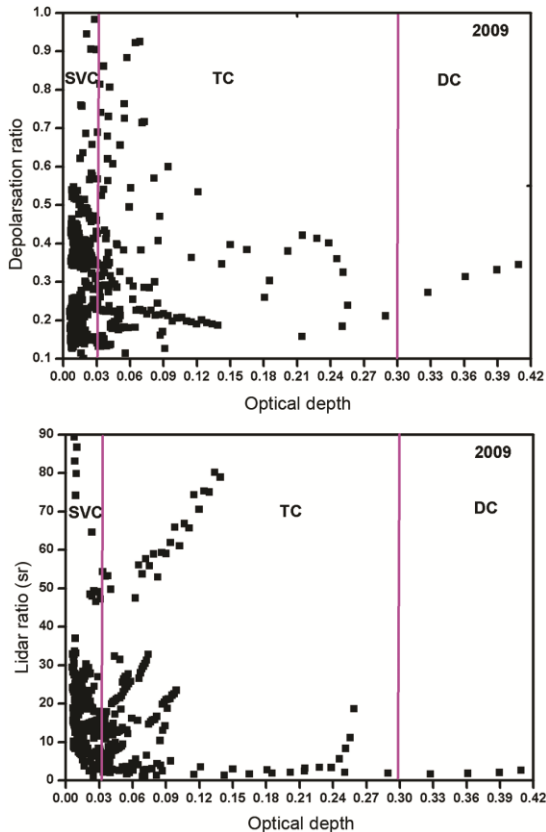
Fig. 11 – Dependence of cirrus optical depth on measured depolarisation ratio and lidar ratio

4.3 Radiative properties of cirrus

Cirrus cloud radiative properties including outgoing long wave radiation (OLR) flux and IR forcing are studied during the period of observation to understand the climate feedback. Depending on the cloud altitude and the optical depth OLR flux will vary for sub-visual, thin and dense cirrus which attribute for the variation in IR forcing. Figure 12 presents the OLR flux and IR forcing of cirrus clouds during the cirrus occurrence days along with cloud optical depth. From figure it is clear that cirrus IR forcing have a strong correlation with optical depth. It is observed that OLR flux is ~460 W/m^2 for SVC and TC with a small difference and show a decrease in the month between June−September to ~345 W/m^2, which correspond to SW monsoon period where the DC is formed with high optical depth. For the NE monsoon and winter again the OLR flux is high where TC is formed. Also it is observed that OLR decreases with increase in optical depth which shows anti-correlation between them.

Cirrus IR forcing shows a strong positive correlation with optical depth. Cirrus IR forcing varied from 3.13 to 110.5 W/m^2 with a mean value of 20.46±8 W/m^2. The positive increasing of cirrus IR forcing shows the greenhouse effect of the clouds leading to a warming of the climate system. Optically

Table 3 − Statistics for cirrus clouds optical properties observed during the period of observation

Type of cirrus	Optical properties	Observed values	Mean
SVC ($\tau_c < 0.03$)	Extinction coefficient, α (m^{-1})	$(2.43–15.32) \times 10^{-6}$	$(6.5 \pm 4.8) \times 10^{-6}$
	Optical depth, τ_c	0.01-0.02	0.02±0.01
	Depolarisation ratio, LDR	0.12-0.59	0.35±0.200
	Lidar ratio, LR	5.6-12.17	8.86±2.43
TC ($0.03 < \tau_c < 0.3$)	Extinction coefficient, α (m^{-1})	$(8.11–67.84) \times 10^{-6}$	$(20.5 \pm 21.14) \times 10^{-6}$
	Optical depth, τ_c	0.03-0.07	0.04±0.01
	Depolarisation ratio, LDR	0.45-1.09	0.57±0.23
	Lidar ratio, LR	2.3-51.77	16.9±17.42
DC ($\tau_c > 0.3$)	Extinction coefficient, α (m^{-1})	$(15.5–79.9) \times 10^{-6}$	$(47.7 \pm 45.6) \times 10^{-6}$
	Optical depth, τ_c	0.43-0.47	0.45±0.03
	Depolarisation ratio, LDR	0.29-0.38	0.34±0.06
	Lidar ratio, LR	5.98-10.25	8.12±3.01
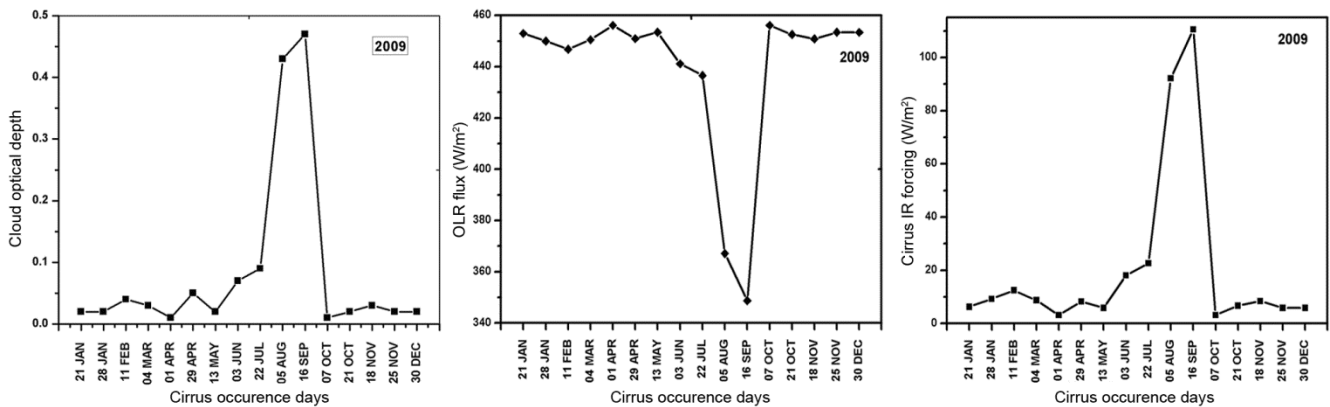
Fig.12 − Variation of cirrus cloud optical depth, OLR and IR forcing during the cirrus occurrence days

thin cirrus clouds usually cause positive radiative forcing at the top of the atmosphere and they warm the climate system, which is in agreement with our results. From Fig. 12 it reveals that the observed values of cirrus IR forcing for SVC is < 7 W/m^2, for TC it ranged from 7 to 25 W/m^2 and for DC >80 W/m^2. The results obtained are in agreement with Das et al.[21]

Radiatively significant clouds should have cirrus IR forcing > 10 W/m^{2,10,30}. From the monthly mean values of cirrus optical depth and IR forcing it is observed that for the lidar-site Gadanki, the cirrus clouds are radiatively significant when the cloud optical depth exceeds 0.04. About 45% of cirrus formed over the observation site is radiatively significant. This is in agreement with the previous results obtained[10,21,30].

5 Conclusions

Cirrus cloud macrophysical, optical and radiative properties are investigated over a tropical station Gadanki, Tirupati during the period of observation from January to December 2009 using a ground based lidar. The cloud base altitudes have a maximum distribution (25%) at 11 − 12 km. The top altitudes have a maximum distribution at 14 − 15 km. The geometrical thickness was confined to a range of 0.9 − 4.5 km. About 75%, the thickness of cirrus clouds was 1.0–2.7 km. Cirrus clouds detected near the tropopause are usually thin and mostly sub-visual. Cirrus mid-cloud temperature ranged from -85 °C to -28 °C.

Monthly mean extinction, σ ranged from 2.84E-06 to 7.99E-05 m^{-1} with an annual mean of 1.79 ± 2.05E-05 m^{-1} which occurs in the month of October and August. The mean extinction is high in the mid cloud altitude range of 12-13.5 km and above the range the extinction decreases. The cloud optical depth ranged from 0.01-0.47 with a mean value of 0.08 ± 0.13, and the occurrence of SVC, TC and DC are 37.5%, 50% and 12.5%. Optical depth shows a strong dependence with cirrus geometrical thickness and mid-cloud height. Optical depth shows a positive correlation with mid-cloud temperature. Monthly mean LDR ranged

from 0.12-1.09 with annual mean of 0.45±0.21. The wide variations in the LDR are due to the changes in the cloud composition arising from the nucleation process. Monthly mean LR ranged from 2.30-51.77 sr with annual mean of 11.48±11 sr. A positive correlation exists for both optical depth and extinction with the mid-cloud temperature. The lidar ratio shows a scattered behavior with mid-cloud temperature.

Cirrus IR forcing have a strong correlation with optical depth. OLR decreases with increase in optical depth which shows anti-correlation between them. Cirrus IR forcing varied from 3.13 to 110.5 W/m^2 with a mean value of 20.46±8 W/m^2. The positive increasing of cirrus IR forcing shows the greenhouse effect of the clouds leading to a warming of the climate system. Optically thin cirrus clouds usually cause positive radiative forcing at the top of the atmosphere and they warm the climate system. Form the monthly mean values of cirrus optical depth and IR forcing it is observed that for the lidar-site Gadanki, the cirrus clouds are radiatively significant when the cloud optical depth exceeds 0.04. About 45% of cirrus formed over the observation site is radiatively significant.

Acknowledgement

References

1   Liou K N, *Mon Weather Rev,* 114 (1986) 1167.
2   Towmey S, *Atmos Environ*, 25 (1991) 2435.
3   McFarquhar G M, Heymsfield A J, Spinhirne J D & Hart B, *J Atmos Sci,* 57 (2000) 184.
4   Heymsfield A J & McFarquhar G M, in *Mid-latitude and tropical cirrus*, edited by Lynch D K, (Oxford UnivPress, New York), 2002, 78.
5   Stephens G L, Tasy S C, Stackhouse P W & Flatau P J, *J Atmos Sci,* 47 (1990) 1742.
6   Chen T, Rossow W B & Zhang Y, *J Clim*, 13 (2000) 264.
7   Fu Q & Liou K N, *J Atmos Sci,* 50 (1993) 2008.
8   Jensen E J, Toon O B, Selkirk H B, Spinhirne J D & Schoberl M A , *J Geophys Res,* 101 (1996) 21361.
9   Sassen K & Campbell J R, *J Atmos Sci,* 58 (2001) 481.
10 Comstock J M & Ackerman T P, *J Geophys Res*, 107 (2002) 4714.
11 Seifert P, Ansmann A, Muller D, Wandinger U, Althausen D, Heymsfield A J, Massie S & Schmitt T, *J Geophys Res,* 112 (2007).
12 Kumar Sunil & Parameswaran S V, *J Geophys Res Atmos*, 110 (2005).
13 *IPCC, Climate change 2007*, edited by Solomon S, (Cambridge University Press, Cambridge, United Kingdom and New York, NY, USA), 2007, 996.
14 Klett J D, *Appl Opt,* 20 (1981) 211.
15 Sassen K & Cho B S, *J Appl Meteorol*, 31 (1992) 1275.
16 Sassen K, *Meteorol Soc,* 72 (1991) 1848.
17 Kumar Sunil, Parameswaran K S V & Krishna Murthy, *Atmos Res*, 66 (2003) 203.
18 Satyanarayana M, Radhakrishnan S R, Veerabhuthiran S, Mahadevan Pillai V, Presennakumar B, Murty V S & Raghunath K, *J Appl Remote Sens*, 4 (2010) 43503.
19 Ackerman T P, Liou K N & Valero F P J, *J Atmos Sci,* 45 (1988) 1606.
20 Spinhirne J D, Hart W D & Hlavka D L, *J Atmos Sci*, 53 (1996) 1438.
21 Das S K, Chiang C W & Nee J B, *Atmos Res*, 93 (2009) 723.
22 Norris J R, *J Geophys Res*, 110 (2005).
23 Platt C M R, Spinhirne J D & Hart W D, *J Geophys Res,* 94 (1989) 11151.
24 Boehm M T, Verlinde J & Ackerman T P, *J Geophys Res*, 104 (1999) 24423.
25 Sassen K, *Rev Laser Eng,* 23 (1995)148.
26 Heymsfield A J & Platt C M R, *J Atmos Sci,* 41 (1984) 846.
27 Platt C M R, Scott J C & Dilley A C, *J Atmos Sci,* 44 (1987) 729.
28 Giannakaki E, Balis D S, Amiridis V& Kazadzis S, *Atmos Chem Phys*, 7 (2007) 5519.
29 Sassen K, Wang Z, Platt C M R & Comstock J M, *J Atmos Sci,* 60 (2003) 428.
30 Brown P R A, Illingworth A J, Heymsfield A J, McFarquhar G M, Browning K A & Gosset M, *J Appl Meteorl*, 34 (1995) 2346.